International Journal of Engineering Research & Technology (IJERT)
ISSN: 2278-0181
Vol. 2 Issue 11, November - 2013

Experimental Study on Flapping Wings at Low Reynolds Numbers

S. Kishore Kumar, M.Tech
Department of Aeronautical Engineering
CMR Technical Campus, Hyderabad, Andhra Pradesh, India

K. Vijayachandar, Ms
Department of Aeronautical Engineering
CMR Technical Campus, Hyderabad, Andhra Pradesh, India

Abstract

The flow field associated with a model flapping wing is studied using low speed wind tunnel. Aerodynamics forces associated with the flow is measured directly with a wind tunnel. The mechanical models replicating the flapping motion of insects have been built and experiments are performed with no forward velocity. 3D component balances to understand the three dimensional flow field and thus underlying mechanisms for the lift and drag produced during a full cycle. The lift was found to be a more dependent on the frequency and the thrust is more dependent of wing span size. Strong span wise velocity components have been found above and below the wing which adds up to thrust in upstroke and lift in the down stroke.

The aerodynamic forces are measured for the designed model with flapping and without flapping at different velocities and compared. The lift and drag changes with upstroke and down stroke are measured and compare the changes in parameters. The respective Reynolds numbers for obtained free stream velocities are calculated.

1. Introduction

Insects have advanced flight control mechanisms that allow them to perform a wide range of manoeuvres. The mechanisms that allow flight of insects and birds are very complicated. Many experiments have been performed to understand the physics involved in creating lift and manoeuvrability of flapping wing animals. Due to the complexity of mimicking natural flapping motion, human built flapping wing aircraft are uncommon and underdeveloped. During flapping flight, insect's wings produce more lift than during steady motion (conventional aerodynamics) at same velocities and angle of attack. (Ref. Cp Ellington). The conventional aerodynamics fails since it is limited to steady wing flight whereas in the case of insect flight, the flow mechanisms are basically unsteady and more complex in nature. There exist certain differences between bird flight and insect flight because of the different flow parameters they belong to like Reynolds number or flapping frequency size, quasi steady or unsteady etc. Insects use an exoskeleton wing which produces unsteady motion effects to sustain flight at low Reynolds number as compared to a bird which uses an endoskeleton wing accompanied with changing wing patterns to produce the required propulsive force. It has been shown that conventional aerodynamic theory, which was based on steady flow conditions, cannot explain the generation of large lift by the wings of small insects. Birds flight is quasi steady as a lot of it involves normal gliding whereas insects are totally in unsteady regime. In the past few years, much progress has been made in revealing the unsteady high-lift mechanisms of flapping insect wings. Highly intensive studies have been done to understand the phenomenon behind insect flight

1.2 AERODYNAMICS OF FLAPPING WING

Flying birds flap their wings to generate lift and thrust as well as to perform remarkable maneuvers with rapid accelerations and decelerations. Insects, bats and birds provide illuminating examples of unsteady aerodynamics. Then, we present a review of nonstationary airfoil aerodynamics including dynamic stall, vortex shedding and thrust generation; followed by a presentation of flapping wing flight in terms of Reynolds number and reduced frequency. Finally, we discuss the flapping wings performance parameters.

1.3 UNSTEADY MECHANISMS IN INSECT FLIGHT

The flapping flight flow is incompressible, highly viscous unsteady, and occurs at low Reynolds numbers. Insect wings with short stroke lengths generate forces much higher than their quasi-steady equivalents due to the presence of unsteady aerodynamic effects. Under steady-state conditions, the high angles of attack at which flapping insect wings operate would normally stall the wings and give deteriorated aerodynamic performance. In practice, however, these wings continue to produce favourable forces even in these extreme conditions.

1.3.1 DELAYED STALL AND THE LEADING EDGE VORTEX

Although a number of unsteady aerodynamic phenomena pertaining to insect like flapping flight have been identified above, they are still unable to explain the high lift required to sustain flight. This remained a mystery essentially until 1996 when Ellington and his co-workers discovered the leading- edge vortex (Ref. Sane 2003).

As the wing increases its angle of attack, the fluid stream going over the wing separates as it crosses the leading edge but reattaches before it reaches the trailing edge. In such case a leading edge vortex (LEV) occupies the separation zone above the wing. Because the flow reattaches, the fluid continues to flow smoothly and the Kutta condition is maintained. In this case, because the wing translates high angle of attack, a greater downward momentum is imparted to the fluid, resulting in substantial enhancement of lift. So the LEV is a region of low pressure above the wing, and this provides an extra suction that increases the lift. The only problem is that the flow continues to feed into the LEV. This would normally cause the vortex to grow so large that it breaks away from the wing, ruining the lift and stalling the wing. However, it has been discovered that the flapping motion causes the LEV to spiral out to the wingtip, siphoning off the vortex and delaying stall. The augmented lift, coupled with the delayed stall, is the principle mechanism that insects use for generating lift.

In forward flight with certain U_∞, for 2-D motion, if the wing continues to translate at high angles of attack, the leading edge vortex grows in size until flow reattachment is no longer possible. The Kutta condition breaks down as vorticity forms at the trailing edge creating a trailing edge vortex as the leading edge vortex sheds into the wake. At this point, the wing is not as effective at imparting a steady downward momentum to the fluid. As a result, there is a drop in lift, and the wing is said to have stalled. For several chord lengths prior to the stall, however, the presence of the attached leading edge vortex produces very high lift coefficients, a phenomenon termed „delayed stall" (Fig 1.3A).

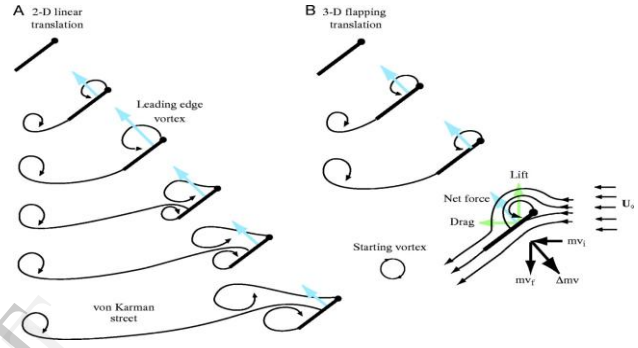

Fig 1 comparison of 2-D linear translation vs 3-D flapping translation (Ref. Sane 2003)

In fig 1.3 (A) 2-D linear translation is shown. As an airfoil begins motion from rest, it generates a leading and trailing edge vortex. During translation, the trailing edge vortex is shed, leading to the growth of the leading edge vortex, which also sheds as the airfoil continues to translate. This motion leads to an alternate vortex shedding pattern from the leading and trailing edges, called the von Karman vortex street

This leads to a time dependence of the net aerodynamic forces (blue arrows) measured on the airfoil. (B) 3-D flapping translation. As in A, when an airfoil undergoing flapping translation starts from rest, it generates a leading and trailing edge vortex. However, as the motion progresses, the leading edge vortex attains a constant size and does not grow any further. Because no new vorticity is generated at the leading edge, there is no additional vorticity generated at the trailing edge and the airfoil obeys the Kutta condition. When established, the Kutta condition ensures that there is a net change in the direction of momentum resulting in a reactive aerodynamic force on the airfoil (black arrows; mv_i signifies initial momentum, mv_f signifies final momentum and Δmv signifies the difference between initial and final momentum). After establishment of the Kutta

condition, the measured net aerodynamic forces (blue arrows) stay stable over a substantial period during translation and do not show time dependence. For Reynolds numbers of ≥100, this force acts normally to the wing and can be decomposed into mutually orthogonal lift and drag components (green arrows). Ultimately, 10 however, the net downward momentum imparted by the airfoil to the fluid causes a downwash that slightly lowers the constant value of the net aerodynamic force on a steadily revolving wing.

Vortices formed are known as the "von Karman vortex street" (Fig 1.1A). The forces generated by the moving plate oscillate in accordance to the alternating pattern of vortex shedding. Although both lift and drag are greatest during phases when a leading edge vortex is present, forces are never as high as during the initial cycle.

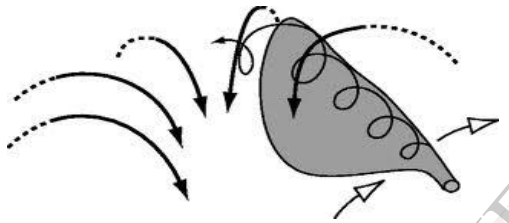

Figure 1.1

1.3 KRAMER EFFECT (Rotational forces)

In other words, the wing generates a rotational circulation in the fluid to counteract the effects of rotation. The re-establishment of Kutta condition is not instantaneous, however, but requires a finite amount of time. If, in this time, the wing continues to rotate rapidly, then the Kutta condition may never be actually observed at any given instant of time during the rotation but the tendency of the fluid towards its establishment may nevertheless dictate the generation of circulation. Thus, extra circulation proportional to the angular velocity of rotation continues to be generated until smooth, tangential flow can be established at the trailing edge. Depending on the direction of rotation, this additional circulation causes rotational forces that either add to or subtract from the net force due to translation. This effect is also often called the „Kramer effect", after M. Kramer who first described it (Kramer, 1932), or alternatively as „rotational forces" (Sane and Dickinson, 2002).

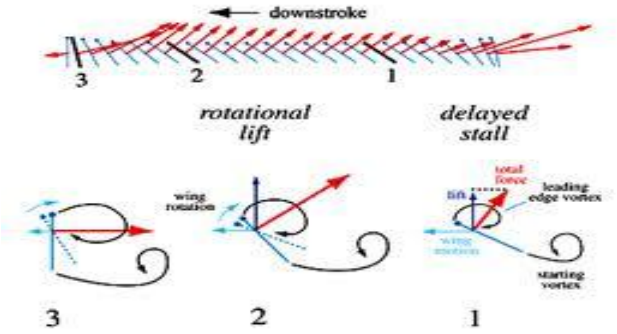

Fig 1.2 Kramer effect (rotational forces)

1.3.2 APPARENT MASS EFFECTS

As an object moves through an inviscid fluid at constant velocity, the fluid ahead of it moves aside and closes up behind it (Ref. Messy 1989). The kinetic energy expended in the process is recovered at the end of it as nothing is lost to viscous drag. If the object now accelerates, not all of the energy expended in parting the flow ahead is recovered when the flow closes up behind it. This additional force required to accelerate the neighbouring fluid around the object is called an apparent mass force. In insect flapping, the fluid around the wing is continually being accelerated or decelerated and these apparent mass forces can be significant. This effect increases with frequency which is higher in insects.

1.4 SCALES AND GOVERNING EQUATIONS

The flows around birds and insects can be considered incompressible: The Mach number is typically 1/300 and the wing frequency is around 10-103 Hz. The governing equation is the Navier–Stokes equation subject to the no slip boundary conditions.

$$\frac{\partial u}{\partial y} + (u.\nabla)u = -\frac{\nabla p}{\rho} + v\nabla^2 u \qquad (1)$$

$$\nabla.u = 0 \qquad (2)$$

$$u_{bd} = u_s \qquad (3)$$

Where u(x, t) is the flow field, p the pressure, ρ the density of the fluid, *v* the kinematic viscosity, u_{bd}

the velocity at the boundary, and u_s is the velocity of the solid. By choosing a length scale, L, and velocity scale, U, the equation can be expressed in non-dimensional form containing the Reynolds number

. $$\mathrm{Re} = \frac{\rho v l}{\mu}$$

The wing area has been found to be proportional to $m^{2/3}$ on an average over the different wing size range, where *m* is the body mass of flying insects, whereas flapping frequency is inversely proportional to the size of the wing (C.P.Ellington, Dudley 2000). Reynolds number Re is the scaling parameter for the insects flapping flight. In unsteady regime, the forward velocity is nearly negligible, for hovering the mean **Re** can be defined on the basis of mean chord $\bar{C} = \frac{2R}{AR}$ mean wing tip velocity

$$\overline{U_t} = 2\phi f \mathrm{R} \qquad (4)$$

$$\mathrm{Re} = \frac{\bar{c}\overline{U_t}}{v} = \frac{4\phi f R^2}{v\mathrm{AR}} \qquad (5)$$

Where f is the wing beat frequency, R is the wing length and Φ is the wing beat amplitude in radians, AR is the aspect ratio. Given the geometric similarity and scaling of frequency, Re is found to increase by m0.42. For larger insects, Re varies from 5000 to 10,000, and it approaches 10 for the smallest ones (C.P.Ellington, 2002). Thus the coefficients of lift and thrust for such cases are defined as

$$C_L = L/0.5A\rho U^2 \qquad (6)$$

$$C_T = T/0.5A\rho U^2 \qquad (7)$$

Where *L* is the lift force, *T* is the thrust force, A is the plan form area of the wing, ρ is the density of air, U is the tip velocity of the wing as given by Eq (3.1).

It is more useful for comparative purposes to introduce a dimensionless measure of speed: the flight velocity divided by the flapping velocity. By analogy to propeller theory, we call this the advance ratio denoted here onwards as J. It is similar to the tip speed ratio of a propeller. The flapping velocity varies linearly along the wing, and some representative value must be chosen to calculate the advance ratio. Again, we choose the mean wingtip flapping velocity, and the advance ratio *J* is then:

$$J = \frac{V}{2\phi n R} \qquad (8)$$

Where V is the forward velocity, R is the wing length and Φ is the wingbeat amplitude in radians, n is the frequency of flapping. The advance ratio is zero during hovering and rises to 0.6 at high speeds for most insects (bumblebees). At first the advance ratio appears to be the inverse of the reduced frequency (k). However, by incorporating the wing span, it more accurately accounts for the 3-D nature of the flows, since longer wing spans corresponds to higher wing tip velocities and generally more unsteadiness. The breakpoint between quasi-steady and unsteady flow is J=1. For J>1 the flow can be considered to be quasi-steady, while for J<1 corresponds to unsteady flow regimes. Most insects operate in this unsteady regime.

1.5 LIFT GENERATION MODEL

Rayner (1979) proposed a model whereby the forces on the wing could be calculated from the nature of the unsteady wake trailing the wing as they flapped. He assumed that rigid wings generated lift only during the down stroke. Thus a series of elliptical vortex rings forms the wake with one vortex ring created during each down stroke. From the Kutta-Juokowski theorem, the lift on a 2-D section of the wing with free stream density of ρ_∞, a free stream speed of U_∞ , and a circulation distribution around the wing of $\Gamma(y)$ is

$$L(y) = \rho_\infty U_\infty \Gamma(y)$$

And hence total lift is given by

$$L = \int_{-b/2}^{b/2} \rho_\infty U_\infty \Gamma(y) dy \qquad (9)$$

The total drag is

$$D = \int_{-b/2}^{b/2} \rho_\infty w(y) \Gamma(y) dy \qquad (10)$$

Where w is the velocity induced by the vortex.

Imposing the Kutta condition, which requires that the flow meets smoothly at the trailing edge without any velocity discontinuities, uniquely

determines the value of circulation $\Gamma(y)$ for the wing and therefore the lift. In order to relate $\Gamma(y)$, the wing circulation to the wake circulation $\Gamma_w(y)$ we make use of the Kelvin's Circulation Theorem

$$\frac{D\Gamma}{Dt} = 0 \qquad (11)$$

Thus if the wing starts from rest, the total circulation is zero and must be so at all times. Therefore any $\Gamma(y)$ generated on the wing must be matched by an equal and opposite $\Gamma_w(y)$ in the wake. Hence $\Gamma(y) = -\Gamma_w(y)$. By using this relation, the lift and drag on the wing can be calculated from the circulation in the wake.

1.6 Force and moment measurement

Experiment 1

C.G of the designed model is calculated as per the dimensions of the model. Fix the model at the C.G and connect it to the holder Switch on the motor of the model to start flapping Switch on motor of the wind tunnel to carry out the experiment for the designed model. The flow over the flapping model is visualised and the performance parameters such as lift, drag moment are calculated. The change in lift and drag with the stroke change are also noted and compare the results. Repeat the experiment for different velocities Calculate the forces and moments at respective velocities. And tabulate the measured values. Plot the graphs for the tabulated values.

Experiment 2

Calculate the C.G for designed model. Fix the model in test section of the wind tunnel. Test the design as a fixed one without flapping. And repeat the experiment as same as the above one. Calculate the performance parameters for desired velocities. Tabulate the results for different velocities. Compare the results with the above experiment and analyze the changes obtained. Reynolds numbers at respective velocities are calculated and tabulate the results. Graphs are plotted for tabulated results.

RESULTS AND DISCUSSION

2 WIND TUNNEL RESULTS

Experimental results obtained by using 3D component balance of wind tunnel. The experiments are performed on flapping wing model. The experiments are performed at different rpm's .3D component balance is used to measure the aerodynamics forces and moments that acts on flapping wing.

Experiment is also performed on fixed wing that is by making wing stationary. The experiments are performed at different rpm's on fixed wing and the aerodynamic forces and moments are calculated by similarly by using 3D component balance.

The results have been compared for different rpm's for both the experiments. It has been observed the change in aerodynamics forces for fixed and flapping wing. In flapping wing lift and drag changes with upstroke and downstroke are compared.

Experimental results for fixed wing

S.No	Lift (L)	Drag (D)	Moment(M)	Velocity(V)
1	-0.05	0.02	0.01	3.89
2	-0.08	0.16	0.01	5.51
3	-0.12	0.18	0.01	6.67
4	-0.15	0.23	0.01	7.80
5	0.07	0.27	0.02	8.71
6	0.08	0.34	0.02	9.54
7	0.10	0.37	0.02	10.31
8	0.11	0.44	0.02	11.02

Table 1.1 lift and drag changes with velocity

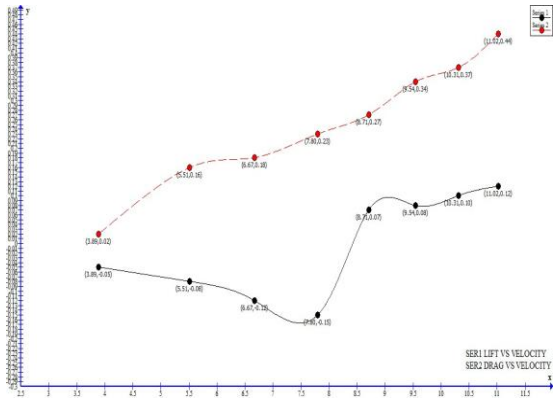

Graph 1.1 lift and drag Vs velocity

Table 1.2 Reynolds number calculation with the velocities obtained

S.No	Velocity	Reynolds number
1	3.89	15.973k
2	5.51	22.625k
3	6.67	27.388k
4	7.80	32.027k
5	8.71	35.764k
6	9.54	39.172k
7	10.31	42.334k
8	11.02	45.249k

Table 1.3 C_L and C_D values at respective lift and drag

S.No	Lift(L)	Coefficient of lift C_L	Drag(D)	Coefficient of drag C_D
1	-0.05	-0.0034	0.02	0.0097
2	-0.08	-0.0028	0.16	0.0037
3	-0.12	-0.0026	0.18	0.0018
4	-0.15	-0.0024	0.23	0.0008
5	0.07	0.00091	0.27	0.0009
6	0.08	0.00086	0.34	0.00086
7	0.10	0.00092	0.37	0.00092
8	0.11	0.00097	0.44	0.00089

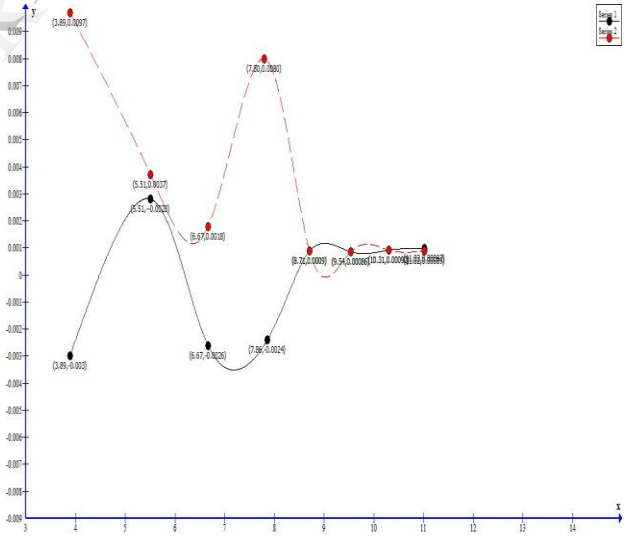

Graph 1.3 C_L and C_D Vs velocity

Experimental results for flapping wing

S.No		(L)	(D)	(M)	(V)
1	Upstroke	-0.11	0.06	0.01	3.89
	Downstroke	0.28	0.02		
2	Upstroke	-0.08	0.16	0.01	5.51
	Downstroke	0.21	0.09		
3	upstroke	-0.12	0.18	0.01	6.67
	Downstroke	0.17	0.11		
4	upstroke	-0.15	0.23	0.01	7.80
	Downstroke	0.15	0.17		
5	Upstroke	0.07	0.27	0.02	8.71
	Downstroke	0.13	0.21		
6	Upstroke	-0.19	0.34	0.02	9.54
	Downstroke	0.12	0.28		
7	upstroke	-0.21	0.32	0.02	10.31
	Downstroke	0.11	0.27		
8	upstroke	-0.27	0.52	0.02	11.02
	Downstroke	0.09	0.32		

Table 1.4 changes in lift and drag at upstroke and down stroke with velocity change

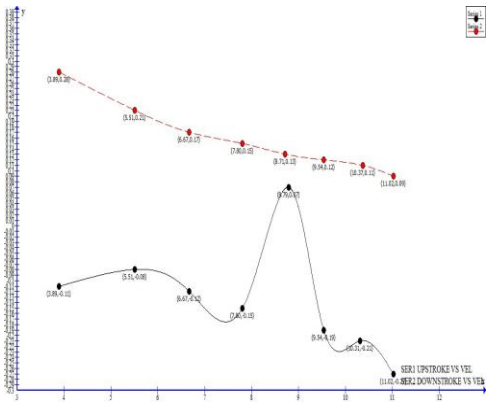

Graph 1.4 changes in lift in upstroke and down stroke with velocity

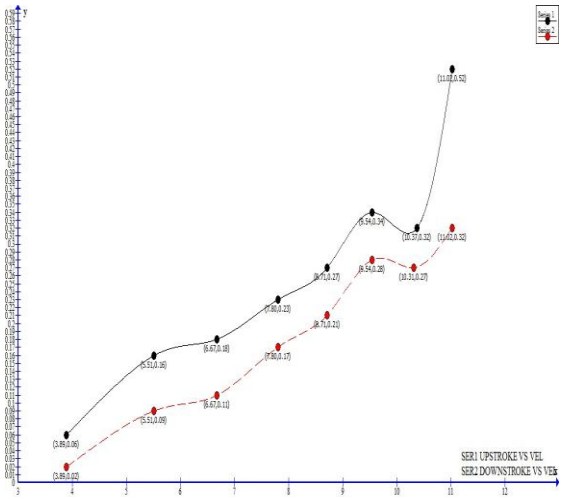

Graph 1.5 change in drag at upstroke and downstroke with velocity

Table 1.5 Shows the values of lift and drag

S.No		Lift(L)	Coefficient of lift C_L	Drag(D)	Coefficient of drag C_D
1	upstroke	-0.11	-0.0071	0.06	0.0039
	downstroke	0.28	0.018	0.02	0.0013
2	upstroke	-0.08	-0.00258	0.16	0.0052
	downstroke	0.21	0.0068	0.09	0.0029
3	upstroke	-0.12	-0.0026	0.18	0.0039
	downstroke	0.17	0.0037	0.11	0.0024
4	upstroke	-0.15	-0.00242	0.23	0.0037
	downstroke	0.15	0.0024	0.17	0.0027
5	upstroke	0.07	0.00091	0.27	0.0058
	downstroke	0.13	0.0017	0.21	0.0045
6	upstroke	-0.19	-0.002	0.34	0.0037
	downstroke	0.12	0.0028	0.28	0.0030
7	upstroke	-0.21	-0.0019	0.32	0.0029
	downstroke	0.11	0.0013	0.27	0.0025
8	upstroke	-0.27	-0.0022	0.52	0.0042
	downstroke	0.09	0.0010	0.32	0.0025

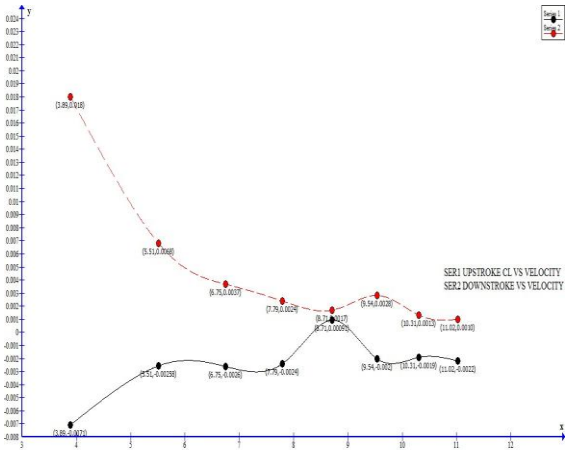

Graph 1.6 changes in C_L at upstroke and down stroke Vs velocity

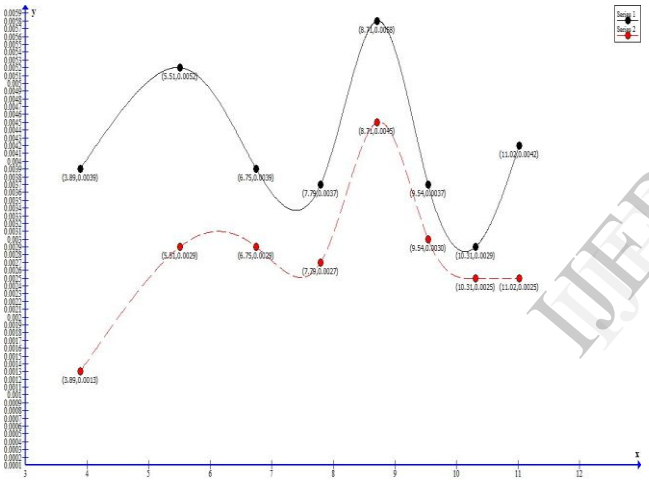

Graph 1.7 shows change in C_D at upstroke and down stroke Vs velocity

CONCLUSION:

Force and moment measurements are carried out to understand the aerodynamics of flapping wing particularly for the insect flight. Air flow around a flapping wing is unsteady because the wing's motion varies continuously. Its Reynolds number is low, typically Re $\approx 10^3$, because of their small size. The Reynolds number based on wing tip velocity and average chord varies between 3414< Re <5690. Since conventional aerodynamics presupposes steady and high Reynolds number flow, it cannot be used directly to analyze insect flight, thus unsteady mechanisms which enhance the aerodynamic force have been studied through experiments. Various models with flapping wing and added features like feathering and lagging are used for experiments. The effect of the different models owing to their overall flapping mechanism is observed. 3 Dimensional unsteady flow fields have been visualized and verified. The variation of forces and flow field with, frequency or model as a whole is studied. In the force measurements section the dependence of aerodynamic forces (lift and thrust) for model 1 over frequency and wing size. And also the variation of velocities the aerodynamic efficiency is calculated for flapping wing model and fixed wing model. These are compared to analyze the unsteady aerodynamics over the designed model. Unsteady flow parameters are calculated and compared with the steady flow parameters. The type of flow patterns are clearly shown with PIV systems which is continued as future work.

REFERENCES

[1] Ansari S.A., R.Z ˙ bikowski, K.Knowles, (2006). "Aerodynamic modeling of insect-like flapping flight for micro air vehicles" Progress in Aerospace Sciences 42, 129–172.
[2] Ellington C. P., (1981). "The Aerodynamics of hovering flight" Phil. Trans. R. Soc. Lond.
[3] Fritz-Olaf Lehmann and Simon Pick (2007). "The aerodynamic benefit of wing–wing interaction depends on stroke trajectory in flapping insect wings" J. of Exp. Biology 212, 1120-1130.
[4] Lehmann, F. O., Sane, S. P. and Dickinson, M. (2005). "The aerodynamic effects of wing-wing interaction in flapping insect wings" J. Exp. Biol. 208, 3075-3092.
[5] Rayner J.M.V., 1979, "A vortex theory of the animal flight. Part 1-2: The vortex wake of a Hovering animal." J Fluid Mechanics 4:697-730, 731-763.
[6] Sane Sanjay P., (2003). "The aerodynamics of insect flight" J. Exp. Biology 206, 4191-4208.
[7] Sane, S. P. and Dickinson, M. H. (2001). "The control of flight force by a flapping wing: lift and drag production" J. Exp. Biol. 204, 2607-2626.
[8] Sane, S. P. and Dickinson, M. H. (2002)."The aerodynamic effects of wing rotation and a revised quasi-steady model of flapping flight" J. Exp. Biol.205, 1087-1096. ake of a Hovering animal." J Fluid Mechanics 4:697-730, 731-763.
[9] Savage, S. B., Newman, B. G. and Wong, D. T.-M. (1979). "The role of vortices and unsteady effects during the hovering flight of dragonflies" J. exp. Biol. 83, 59-77.
Wang Z. J. (2000). "Vortex shedding and frequency selection in flapping flight." J. Fluid Mech. 410, 323-34